

Effective Hamiltonian for edge states in graphene

H. Deshpande¹ and R. Winkler^{1,2}

¹*Department of Physics, Northern Illinois University, DeKalb, Illinois 60115, USA*

²*Materials Science Division, Argonne National Laboratory, Argonne, Illinois 60439, USA*

(Dated: March 14, 2016)

We propose an effective two-band Hamiltonian for the electronic states in graphene based on a Taylor expansion of the tight-binding Hamiltonian about the time-reversal invariant M point at the edge of the Brillouin zone. This Hamiltonian provides an accurate description of the topologically protected edge states for both zigzag and armchair edges in graphene ribbons although the concept of a Brillouin is not part of such an effective model. The model highlights the importance of boundary conditions for the occurrence of edge states. Such states occur for band inversion or a mass domain wall at the edge of the ribbon, but they are absent otherwise.

A topological insulator is an insulator in the bulk with topologically protected edge states that cross the gap so that the edges are conducting. This concept was first introduced by Kane and Mele using a simple tight-binding (TB) model for the band structure of graphene [1, 2]. Since then a wide range of materials with these properties have been identified in two and three dimensions (2D and 3D) [3, 4]. Topological insulators can be distinguished from trivial insulators without topological edge states by the values of one or multiple topological invariants that require an analysis of the bulk band structure across the Brillouin zone. In that sense topological insulators are considered conceptually different from other problems in solid state physics that permit a description local in \mathbf{k} space. A major aspect motivating the interest in topological insulators lies in the fact that elastic backscattering from a random potential is forbidden in these edge states [2].

The first experimental verification of topologically protected edge states was achieved for HgTe/CdTe quantum wells (QWs) [5] following a theoretical proposal by Bernevig, Hughes and Zhang [6] based on a simple effective Hamiltonian, today known as the BHZ model. Since then the BHZ model has been used in a wide range of studies. Liu et al. showed [7] that it also describes the edge states in InAs/GaSb QWs. Zhou et al. showed [8] that the BHZ model can be solved exactly, yielding analytical expressions for the edge states in HgTe/CdTe QWs, see also Ref. 9. Zhou's work [8] raised the question to what extent topological insulators permit a description local in \mathbf{k} space, i.e., using a model not involving the concept of a Brillouin zone. Graphene with its simple TB description [1, 2, 10] has served as an archetype for topological insulators. We show here that a Taylor expansion of the graphene TB model about the time-reversal invariant M point of the Brillouin zone yields an effective Hamiltonian that provides an accurate description local in \mathbf{k} space of the edge states in both zigzag and armchair graphene ribbons.

In the following our conventions for the TB Hamiltonian follow Refs. [1, 2], see also Ref. [11]. While the graphene Brillouin zone has two inequivalent points K and K' , we have three inequivalent points M , M' and

M'' , see Figs. 1(c) and 1(d). Expanding the TB Hamiltonian for the graphene π bonds about $\mathbf{M}'' = (0, 2\pi/\sqrt{3})$ as in Fig. 1(d), the effective Hamiltonian up to second order in $\mathbf{k} = (k_x, k_y)$ becomes

$$H_M(\mathbf{k}) = \left[\left(1 - \frac{1}{4}k_x^2 + \frac{1}{12}k_y^2 \right) \sigma_z + \frac{2}{\sqrt{3}}k_y\sigma_y \right] t - \sigma_x\lambda_v \\ - 4k_x s_z \sigma_x \lambda_i + \left[-\frac{2}{\sqrt{3}}s_x \sigma_y - \left(\frac{1}{2\sqrt{3}}k_y s_x + \frac{\sqrt{3}}{2}k_x s_y \right) \sigma_z \right. \\ \left. + \left(\frac{1}{8}k_x^2 s_x - \frac{1}{4}k_x k_y s_y + \frac{5}{24}k_y^2 s_x \right) \sigma_y \right] \lambda_r \quad (1)$$

where s_i denotes spin operators and σ_i are Pauli matrices referring to a basis that diagonalizes $H_M(\mathbf{k})$ in the limit $\mathbf{k} \rightarrow 0$. The first term describes the orbital motion characterized by the nearest-neighbor hopping parameter t . In the following we assume $t = 1$, i.e., we measure all energies in units of t . Similarly, lengths are measured in units of the lattice constant a . The second term describes a staggered sublattice potential weighted by λ_v [1, 2]. The third term gives the intrinsic spin-orbit (SO) coupling proportional to the parameter λ_i . The fourth term describes the Rashba SO coupling weighted by the parameter λ_r .

First we discuss the properties of the Hamiltonian (1) in the absence of SO coupling. Unlike the Bloch states at the K point [12], the Bloch states at the M point [i.e., the eigenstates of the Hamiltonian (1) for $\mathbf{k} = 0$ which are eigenstates of the Pauli matrix σ_z] are nonzero on both sublattices A and B of the graphene structure (with equal weights for A and B) so that here σ_z does not permit an interpretation as sublattice pseudospin. For $\lambda_v = 0$, the dispersion becomes

$$E_{\pm}(\mathbf{k}) = \pm \sqrt{\left(1 - \frac{1}{4}k_x^2 \right)^2 + k_y^2 \left(\frac{3}{2} - \frac{1}{24}k_x^2 \right) + \frac{1}{144}k_y^4} \quad (2)$$

where the upper (lower) sign corresponds to the conduction (valence) band. For these bands the M point is not an extremal point but a saddle point. For $k_x = 0$, the dispersion becomes $E_{\pm}(0, k_y) = \pm \sqrt{1 + \frac{3}{2}k_y^2 + \frac{1}{144}k_y^4}$. In the perpendicular direction $k_y = 0$ we get $E_{\pm}(k_x, 0) = \pm \left(1 - \frac{1}{4}k_x^2 \right)$ so that the bands touch at the points $(\pm 2, 0)$, which mimics the dispersion near the points K and K' of the Brillouin zone, the precise coordinates of which are $(\pm 2\pi/3, 0)$. Indeed, if we substitute $k_x \rightarrow k_x \pm 2$, the

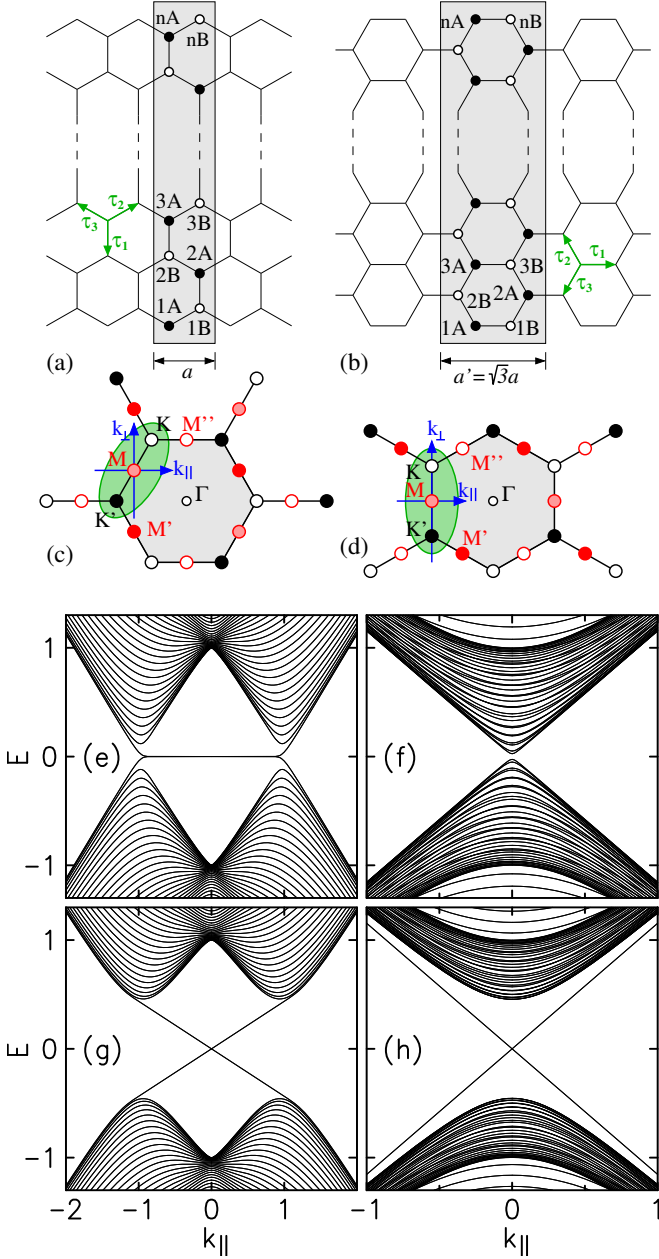


FIG. 1. (Color online) Crystal structure of a graphene ribbon with (a) zigzag and (b) armchair edges for width n . The shaded areas denote the unit cell. Bulk Brillouin zone of graphene corresponding to (c) zigzag and (d) armchair ribbons. The region of the Brillouin zone captured by the Hamiltonian (1) is marked in green. Band structure $E(k_{\parallel})$ of (e) zigzag and (f) armchair ribbons in the absence of SO coupling and (g), (h) for $\lambda_i = 0.2$. The width of the ribbons is $w = 40$ and we used $b_v = -10$.

Hamiltonian (1) is unitarily equivalent to

$$H_K(\mathbf{k}) = \pm k_x \sigma_x - \frac{2}{\sqrt{3}} k_y \sigma_y + \left(\frac{1}{4} k_x^2 - \frac{1}{12} k_y^2 \right) \sigma_x + \lambda_v \sigma_z \pm 4(2 \pm k_x) s_z \lambda_i \sigma_z \quad (3)$$

where we also included the sublattice staggering $\propto \lambda_v$

and the intrinsic SO coupling $\propto \lambda_i$ for later reference. For small \mathbf{k} , Eq. (3) is close to the Dirac Hamiltonian $H_D = \frac{\sqrt{3}}{2}(\pm k_x \sigma_x - k_y \sigma_y)$ obtained via a Taylor expansion of the TB Hamiltonian about K and K' [13]. The Hamiltonian (1) thus captures the essential features of the graphene multivalley band structure for both the conduction and valence band near the entire line $K - M - K'$. Recently multivalley band structures such as the one realized in graphene have attracted significant interest in the context of *valleytronics*. Here multiple valleys are usually described as replicas of a single-valley Hamiltonian using a valley-pseudospin as a separate degree of freedom [14], which corresponds to the two signs in H_D . The multivalley Hamiltonian (1) thus provides an alternative approach to such scenarios, using nonetheless the powerful language of effective Hamiltonians. We note that the Hamiltonian (1) accounts for time reversal symmetry in a natural way, which reflects the fact that the M point used here as expansion point is known as time-reversal invariant momentum [15]. We also note that it follows immediately from Eq. (3) that $\lambda_v \neq 0$ opens a gap $2|\lambda_v|$ at $\mathbf{k} = (\pm 2, 0)$.

To discuss edge states we consider graphene ribbons with so-called zigzag [Fig. 1(a)] and armchair edges [Fig. 1(b)]. The bulk band structure of the 1D ribbons can be obtained by projecting the bulk band structure of 2D graphene on the axis along the ribbon. It follows that the electronic states in these ribbons around energy $E = 0$ emerge from the states in 2D graphene which are highlighted in green in Fig. 1(c) and (d).

First we focus on zigzag edges [Fig. 1(a)]. We denote the wave vector for the unconfined motion along the direction of the ribbon as k_{\parallel} and the perpendicular component as k_{\perp} . Ignoring SO coupling, zigzag edges give rise to a gapped spectrum around $k_{\parallel} = 0$ with edge states appearing in the center of the gap [16]. These results are readily rederived by means of Hamiltonian (1), where a suitable coordinate transformation gives the Hamiltonian

$$H_z(\mathbf{k}) = \left(1 - \frac{1}{6} k_{\perp}^2 + \frac{1}{2\sqrt{3}} k_{\perp} k_{\parallel} \right) \sigma_z - \left(\frac{1}{\sqrt{3}} k_{\perp} + k_{\parallel} \right) \sigma_y \quad (4)$$

Note that the expansion point $k_{\parallel} = 0$ for the effective Hamiltonian (4) corresponds to the point $\tilde{k}_{\parallel} = \pi$ of the 1D Brillouin zone for zigzag ribbons [see, e.g., Fig. 2(b) in Ref. 16].

We assume as in Refs. 1, 2, and 16 that the edges are interfaces towards vacuum. Within the framework of effective Hamiltonians, we use the Hamiltonian (4) for both graphene and vacuum with suitable distinct band parameters for each region, combined with the usual matching conditions at the interfaces to ensure hermiticity of the resulting eigenvalue problem [17, 18]. For conceptual simplicity we vary only one band parameter across the graphene-vacuum interface, either the gap or the prefactor of the term $\propto k_{\perp}^2 \sigma_z$. In either case, this is done symmetrically for both spinor components so that we preserve the electron-hole symmetry in the spectrum of the Hamiltonian. In the end we may consider the limit where

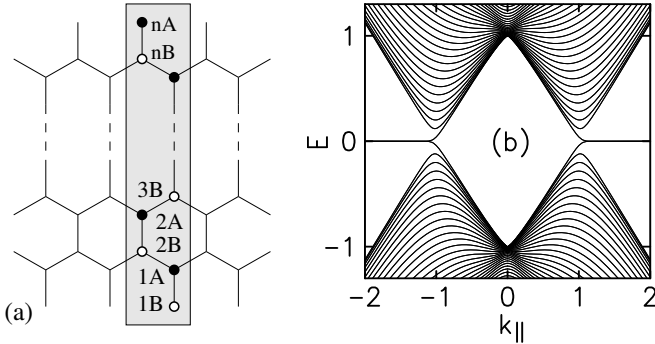


FIG. 2. Crystal structure of a graphene ribbon with “dangling” zigzag edges for width n . The shaded areas denote the unit cell. (b) Band structure $E(k_{\parallel})$ of the ribbon in the absence of SO coupling. The width of the ribbons is $w = 40$ and we used $b_v = +10$.

these band parameters for vacuum are chosen such that the graphene wave functions vanish at the interface.

The edge states obtained by means of Hamiltonian (4) are shown in Fig. 1(e). In these calculations, we confined the electrons inside the graphene ribbon by adding the term $b\sigma_z$ to the Hamiltonian (4) with $b \equiv b_g = 0$ inside the graphene ribbon and $b \equiv b_v = -10$ in vacuum. Having $b_v < 0$ implies a band inversion at the graphene-vacuum interface [19]. A simple confinement $b_v > 0$ results in the spectrum shown in Fig. 2(b), where we have the same bulk spectrum as in Fig. 1(e), but the edge states appear for $|k_{\parallel}| > 1$. The latter type of spectrum is obtained in TB calculations for ribbons with “dangling” zigzag edges [20], see Fig. 1(b). We have thus a direct correspondence between the boundary conditions in a TB description of graphene ribbons and the boundary conditions for the effective Hamiltonian used here. In our approach we may alternatively describe the interface via a position-dependent prefactor μ for the term $\propto k_{\perp}^2 \sigma_z$. Again the bulk spectrum of the ribbon does not depend on the sign of μ in vacuum. But edge states as in Fig. 1(e) occur only for a sign change of μ corresponding to a mass domain wall at the interface [21, 22], whereas without a sign reversal of μ we obtain a spectrum as in Fig. 2(b). Either band inversion or a mass domain wall are thus required to obtain edge states near $k_{\parallel} = 0$. In that sense these requirements may be considered here as equivalent for the occurrence of edge states. In the following we focus on $b_v < 0$.

The numerical calculations presented in this work use a quadrature method as described in Refs. 23 and 24, which automatically ensures the proper matching conditions for the multi-spinor wave function at the graphene-vacuum interface. The numerical results can be confirmed by analytical calculations similar to those in Refs. 8 and 9. In particular, the limit of hard walls $b_v \rightarrow -\infty$ yields for the edge state at $k_{\parallel} = 0$ of a semi-infinite graphene sheet

at $r_{\perp} \geq 0$

$$\psi_z(r_{\perp}) = \begin{pmatrix} 1 \\ 1 \end{pmatrix} (e^{-\kappa+r_{\perp}} - e^{-\kappa-r_{\perp}}), \quad \kappa_{\pm} \equiv \sqrt{3}(1 \pm i) \quad (5)$$

and $\psi_z(r_{\perp} < 0) = 0$. The corresponding eigenenergy is $E = 0$. The full expressions for finite b_v , finite thickness of the ribbon and finite k_{\parallel} are more complicated so that they are not reproduced here. Yet such calculations confirm immediately that no edge states exist around $k_{\parallel} = 0$ for $b_v > 0$.

For a ribbon with armchair edges [Fig. 1(b)] and neglecting SO coupling, the effective Hamiltonian becomes

$$H_a(\mathbf{k}) = \left(1 - \frac{1}{4}k_{\perp}^2 + \frac{1}{12}k_{\parallel}^2\right)\sigma_z - \frac{2}{\sqrt{3}}k_{\parallel}\sigma_y \quad (6)$$

see Fig. 1(d). The 1D spectrum resulting from this Hamiltonian is shown in Fig. 1(f). Here we have no edge states (for either sign of b_v) and in the limit of wide ribbons the spectrum becomes gapless. These results are consistent with the findings in Ref. 16, keeping in mind that the bulk K and K' points are folded to the point $\tilde{k}_{\parallel} = 0$ of the 1D Brillouin zone for armchair ribbons.

Previously Brey and Fertig [25] used the graphene Dirac Hamiltonian H_D to obtain the edge states of 1D ribbons emerging from the states near the K point of 2D graphene [26], i.e., their model gives the edge states for wave vectors close to the valence band maximum and conduction band minimum in Figs. 1(e) and (f). The present approach is different from this earlier work as it yields the edge states in the entire region in between the points K and K' of the bulk band structure, consistent with the TB description [16]. Effective Hamiltonians based on a Taylor expansion of the band structure are often low-energy Hamiltonians that are valid only in the vicinity of the expansion point [17, 18]. Yet this is not an inherent constraint as previously shown by Cardona and Pollak [27] who developed a full-zone $\mathbf{k} \cdot \mathbf{p}$ method for germanium and silicon. The present work follows a similar spirit as Ref. 27 by providing an effective Hamiltonian that is valid for a large range of wave vectors and a large range of energies.

Next we discuss the effect of SO coupling. First we consider $\lambda_r = 0$. The intrinsic SO coupling $\propto \lambda_i$ opens a gap $16\lambda_i\sqrt{1 - 16\lambda_i^2} \approx 16\lambda_i$ in the bulk spectrum of the Hamiltonian (1). In the TB model this gap takes the value $6\sqrt{3}\lambda_i$ [2]. For $\lambda_i \neq 0$ the edge states in a zigzag ribbon remain two-fold degenerate at $k_{\parallel} = 0$ which reflects the fact that these states originate from the time-reversal invariant M point of the graphene Brillouin zone. This aspect is thus readily captured by the Hamiltonian (1) that stems from an expansion about the M point, as demonstrated in Fig. 1(g). For $k_{\parallel} \neq 0$, the two-fold degeneracy is lifted and the branches ultimately merge with the bulk conduction and valence band [1, 2].

Both the intrinsic SO coupling $\propto \lambda_i$ and the sublattice staggering $\propto \lambda_v$ open a gap in the bulk spectrum of the Hamiltonian (1). Yet it follows immediately from

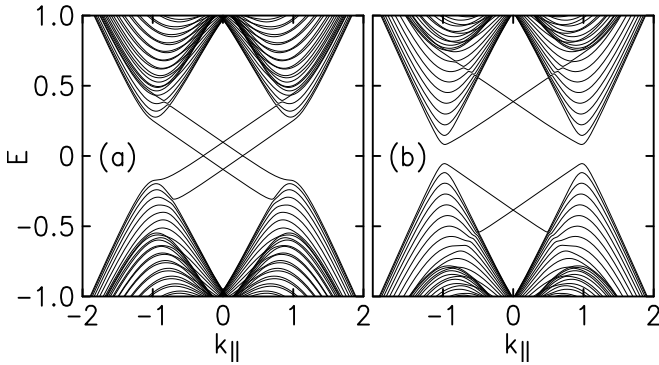


FIG. 3. Band structure $E(k_{\parallel})$ of zigzag ribbons for $\lambda_i = 0.09$ and $\lambda_r = 0.05$. The sublattice staggering is (a) $\lambda_v = 0.1$ and (b) $\lambda_v = 0.4$. The width of the ribbon is $w = 40$ and we used $b_v = -10$. Compare Fig. 1 of Ref. 1.

Eq. (3) that the gap closes for $\lambda_v = \pm 8\lambda_i$. Consistent with the TB results in Ref. [1] this set of parameters describes the phase boundary between the topologically trivial regime with an even number of edge states and the nontrivial regime with an odd number of edge states crossing the bulk gap. Similarly, Rashba SO coupling $\propto \lambda_r$ induces such a phase transition when it competes with the intrinsic SO coupling. We illustrate this point for our approach in Fig. 3 showing two calculations for zigzag ribbons with $\lambda_i = 0.09$ and $\lambda_r = 0.05$. The sublattice staggering $\lambda_v = 0.1$ [Fig. 3(a)] gives rise to edge states crossing the gap, whereas $\lambda_v = 0.4$ [Fig. 3(b)] results in an ordinary insulator, where the edge states do not cross the bulk gap. These calculations are in good agreement with the TB results in Fig. 1 of Ref. 1.

Next we discuss the effect of SO coupling on the spectrum of ribbons with armchair edges. Similar to the band structure of 2D graphene, intrinsic SO coupling opens a gap in the spectrum of armchair ribbons. Furthermore, we obtain edge states in the center of the gap which, for increasing λ_i , develop from the bulk $k_{\parallel} = 0$ states in the absence of SO coupling. The spectrum in Fig. 1(h) is in good agreement with TB calculations analogous to those described in Refs. 1 and 2.

Using an effective Hamiltonian as in Eq. (1) we can readily include a range of perturbations such as homogeneous or inhomogeneous [28] magnetic and electric fields or strain which may break the periodicity of the ideal crystal structure [29]. To illustrate this point we consider a zigzag ribbon in the presence of an exchange field $\lambda_x s_z$ and Rashba SO coupling $\propto \lambda_r$, which gives rise to the quantum anomalous Hall effect [30], see Fig. 4(a). If the exchange field λ_x is due to paramagnetic ions [31], a magnetic field is normally required to induce the ex-

change splitting. Here we incorporate an external magnetic field B_z perpendicular to the plane of the ribbon via the usual Peierls substitution $k_{\perp} \rightarrow k_{\perp} + B_z r_{\perp}$, where r_{\perp} denotes the spatial coordinate conjugate to k_{\perp} . A magnetic field $B_z = 0.02$ significantly distorts the dispersion $E(k_{\parallel})$ [Fig. 4(b)], but the edge states crossing the gap

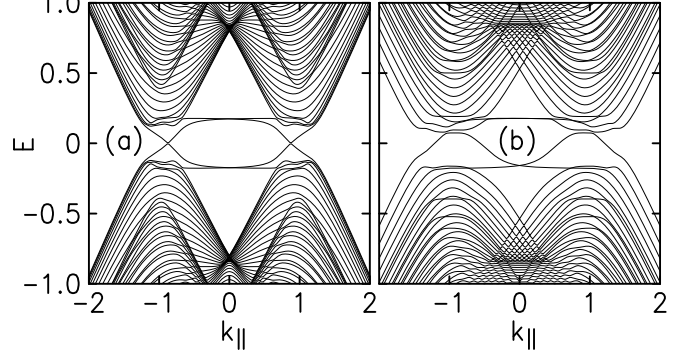


FIG. 4. Band structure $E(k_{\parallel})$ of zigzag ribbons for $\lambda_i = 0.0$, $\lambda_r = 0.1$, $\lambda_x = 0.18$ and (a) magnetic field $B_z = 0$ and (b) $B_z = 0.02$. The width of the ribbon is $w = 40$ and we used $b_v = -10$.

are robust under such a perturbation.

Finally we comment on the general robustness of the edge states, which is a major aspect motivating the interest in topological insulators [3, 4]. It was pointed out in Ref. 2 that the edge states at $\pm k_{\parallel}$ form a Kramers doublet so that elastic backscattering from a random potential preserving time reversal symmetry is forbidden. If the electron states in graphene are modeled by means of the low-energy Dirac Hamiltonian H_D , the two valleys at K and K' are described via a discrete valley pseudospin degree of freedom, that makes it difficult to incorporate intervalley scattering in a general way. For the effective Hamiltonian (1) pairs of time-reversed states are connected by continuous paths in the Hilbert space of this Hamiltonian so that it is well-suited to incorporate intervalley scattering, though a detailed study of this point is beyond the scope of the present work.

In conclusion, the effective Hamiltonian (1) based on an expansion of the graphene TB Hamiltonian about the time-reversal invariant M point provides an accurate description of many facets of the topologically protected edge states in graphene, although the concept of a Brillouin is not part of such an effective model. RW appreciates stimulating discussions with C. S. Chu, C. L. Kane and U. Zülicke. This work was supported by the NSF under grant No. DMR-1310199. Work at Argonne was supported by DOE BES under Contract No. DE-AC02-06CH11357.

[1] C. L. Kane and E. J. Mele, Phys. Rev. Lett. **95**, 146802 (2005).

[2] C. L. Kane and E. J. Mele, Phys. Rev. Lett. **95**, 226801 (2005).

- [3] M. Z. Hasan and C. L. Kane, Rev. Mod. Phys. **82**, 3045 (2010).
- [4] X.-L. Qi and S.-C. Zhang, Rev. Mod. Phys. **83**, 1057 (2011).
- [5] M. König, S. Wiedmann, C. Brüne, A. Roth, H. Buhmann, L. W. Molenkamp, X.-L. Qi, and S.-C. Zhang, Science **318**, 766 (2007).
- [6] B. A. Bernevig, T. L. Hughes, and S.-C. Zhang, Science **314**, 1757 (2006).
- [7] C. Liu, T. L. Hughes, X.-L. Qi, K. Wang, and S.-C. Zhang, Phys. Rev. Lett. **100**, 236601 (2008).
- [8] B. Zhou, H.-Z. Lu, R.-L. Chu, S.-Q. Shen, and Q. Niu, Phys. Rev. Lett. **101**, 246807 (2008).
- [9] E. B. Sonin, Phys. Rev. B **82**, 113307 (2010).
- [10] P. R. Wallace, Phys. Rev. **71**, 622 (1947).
- [11] To match the conventions in Ref. 23, the intrinsic SO term in Eq. (1) must be multiplied by a factor $-1/2\sqrt{3}$ and the Rashba term by $-1/\sqrt{3}$.
- [12] K. S. Novoselov, A. K. Geim, S. V. Morozov, D. Jiang, M. I. Katsnelson, I. V. Grigorieva, S. V. Dubonos, and A. A. Firsov, Nature **438**, 197 (2005).
- [13] A. H. Castro Neto, F. Guinea, N. M. R. Peres, K. S. Novoselov, and A. K. Geim, Rev. Mod. Phys. **81**, 109 (2009).
- [14] J. Tworzydło, I. Snyman, A. R. Akhmerov, and C. W. J. Beenakker, Phys. Rev. B **76**, 035411 (2007).
- [15] L. Fu, C. L. Kane, and E. J. Mele, Phys. Rev. Lett. **98**, 106803 (2007).
- [16] M. Fujita, K. Wakabayashi, K. Nakada, and K. Kusakabe, J. Phys. Soc. Jpn. **65**, 1920 (1996).
- [17] G. Bastard, *Wave Mechanics Applied to Semiconductor Heterostructures* (Les Editions de Physique, Les Ulis, 1988).
- [18] R. Winkler, *Spin-Orbit Coupling Effects in Two-Dimensional Electron and Hole Systems* (Springer, Berlin, 2003).
- [19] B. A. Volkov and O. A. Pankratov, JETP Lett. **42**, 178 (1985).
- [20] B. A. Bernevig, *Topological Insulators and Topological Superconductors* (Princeton University Press, Princeton, NJ, 2013).
- [21] Y.-C. Chang, J. N. Schulman, G. Bastard, Y. Guldner, and M. Voos, Phys. Rev. B **31**, 2557 (1985).
- [22] Y. R. Lin-Liu and L. J. Sham, Phys. Rev. B **32**, 5561 (1985).
- [23] R. Winkler and U. Zülicke, Phys. Rev. B **82**, 245313 (2010).
- [24] R. Winkler and U. Rössler, Phys. Rev. B **48**, 8918 (1993).
- [25] L. Brey and H. A. Fertig, Phys. Rev. B **73**, 235411 (2006).
- [26] Similar to the present work, boundary conditions played also an important role in Ref. 25. Yet the nature of these boundary conditions was very different from the boundary conditions used here. Brey and Fertig treated the vacuum as hard walls. As H_D is linear in momentum we cannot require that both spinor components vanish simultaneously at the boundaries.
- [27] M. Cardona and F. H. Pollak, Phys. Rev. **142**, 530 (1966).
- [28] F. D. M. Haldane, Phys. Rev. Lett. **61**, 2015 (1988).
- [29] G. L. Bir and G. E. Pikus, *Symmetry and Strain-Induced Effects in Semiconductors* (Wiley, New York, 1974).
- [30] Z. Qiao, S. A. Yang, W. Feng, W.-K. Tse, J. Ding, Y. Yao, J. Wang, and Q. Niu, Phys. Rev. B **82**, 161414 (2010).
- [31] C.-X. Liu, X.-L. Qi, X. Dai, Z. Fang, and S.-C. Zhang, Phys. Rev. Lett. **101**, 146802 (2008).